

Energy Efficient Battery Heating in Cold Climates

Andreas Vlahinos

Advanced Engineering Solutions

Ahmad A. Pesaran

National Renewable Energy Laboratory

ABSTRACT

In cold climates batteries in electric and hybrid vehicles need to be preheated to achieve desired performance and life cycle of the energy storage system and the vehicle. Several approaches are available: internal core heating; external electric heating of a module; internal electric heating in the module around each cell, internal fluid heating around each cell; and external fluid heating around each module.

To identify the most energy efficient approach, we built and analyzed several transient thermal finite element models of a typical battery. The thermal transient response of the battery core was computed for the first four heating techniques, which were compared based on the energy required to bring the battery to the desired temperature in a given time. Battery core heating was the most effective method to warm battery quickly with the least amount of energy. Heating the core by applying high frequency alternating currents through battery terminals is briefly discussed.

INTRODUCTION

Battery performance in cold climates is a major concern for electric and hybrid electric vehicles (EVs and HEVs). Warming batteries in HEVs and EVs is necessary to improve their performance in cold temperatures. A major challenge for heating batteries in cold environments is the availability of energy. If the temperature is very low, both the battery and the engine (in an HEV) are cold. No on-board heat is available unless it is stored as thermal energy. Electrical energy from the battery or the on-board generator could also be converted to heat.

The potential heat sources could be 1) heat from the engine for battery heating with a fluid or 2) the electrical energy from the battery or generator. For option 1, the engine performance is sluggish at very cold temperatures

and will take a while to warm up to provide the heat. Therefore option 1 may not work fast enough. In option 2, if there is energy in the battery, drawing power is difficult but power at even low currents can warm the battery since the resistance is so high and thus the resistive heating is high. The engine can also be used to power the on-board generator. A system that uses energy from the battery for warming it has been proposed (Ashtiani and Stuart). For EVs, off-board chargers can be used to heat batteries electrically.

Performance of all batteries decreases with temperature to varying degrees; at very cold temperatures the battery ceases to operate properly, which leads to reduced life. HEVs may suffer even more than conventional vehicles because their batteries perform poorly. Warming up batteries is essential for achieving acceptable power and energy performance from HEV batteries.

The objective of this investigation is to evaluate which method could be more effective for heating HEV batteries in very cold temperatures by performing thermal analysis on four cases shown in Table 1.

Table 1. Preheating Techniques

Case	Preheating Techniques	
1	Internal core heating	Electric heating of battery core in each cell
2	External jacket heating	Heating of external module using electric heaters
3	Internal jacket heating	Heating of external cells using electric heaters
4	Internal fluid heating	Heating using hot fluid around cell

CASE 1: INTERNAL CORE HEATING

FINITE ELEMENT MODELING

The geometry of the battery pack considered was rectangular and had six modules. The approximate external dimensions of the pack and core modulus are shown in Table 2.

Table 2. Pack and Core Dimensions

	Width	Length	Height
Pack	76.20 mm	254.0 mm	127.0 mm
Core	63.50 mm	38.10 mm	114.3 mm

The core, the polypropylene case, and the spacing material properties are assumed to be isotropic and temperature independent. Table 3 shows the properties of all three materials.

Table 3. Material Properties

	Core	Polypropylene	Spacer
Conductivity (W/m K)	15	0.17	0.17
Heat Capacity (J/kg K)	810	910	910
Density (kg/m ³)	2327	1930	1930

A parametric three-dimensional transient thermal finite element model of a typical battery pack was built and analyzed. Figure 1 shows half of the finite element model. Figure 2 shows a detail of Case 1 finite element model with part of the core, plastic case, and contact resistance (or a spacer). As the temperature in the battery core increases, the resistance decreases, leading to lower heat generation. Figure 3 shows the transient volumetric heat generation applied at the battery core versus time for four different power levels. Natural convection was applied on all exterior surfaces. The heat transfer or convection film coefficient for the side surfaces was assumed to be 2.0 W/m² K. The film coefficient for the top surfaces was assumed to be 3.0 W/m² K. The film coefficient for the bottom surfaces was assumed to be 1.0 W/m² K. The environment (bulk temperature for all convection surfaces) and initial module temperature were considered to be -40°C.

INTERNAL CORE HEATING RESULTS

Temperature increases with time and the amount of internal heating energy. Figure 4 shows a small non-uniform temperature distribution at 10 minutes. The interior cells are warmer than the exterior ones.

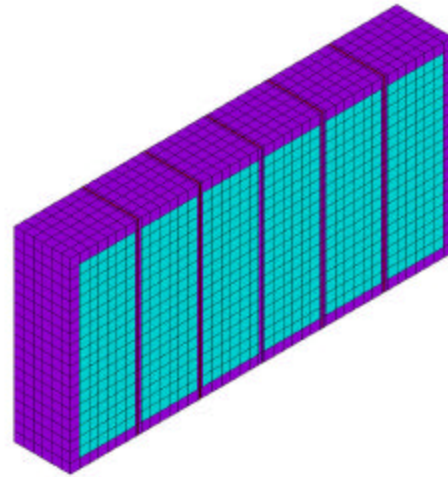


Figure 1. Half of finite element model for Case 1

The maximum core temperature versus time is shown in Figure 5. After 2 minutes the slope of temperature rise decreases because of lower heating energy applied (see Figure 3). The effect of input energy on temperature rise for 1, 3, 6, and 10 minutes is shown in Figure 6. The temperature rises linearly versus time with different slopes depending on input energy level.

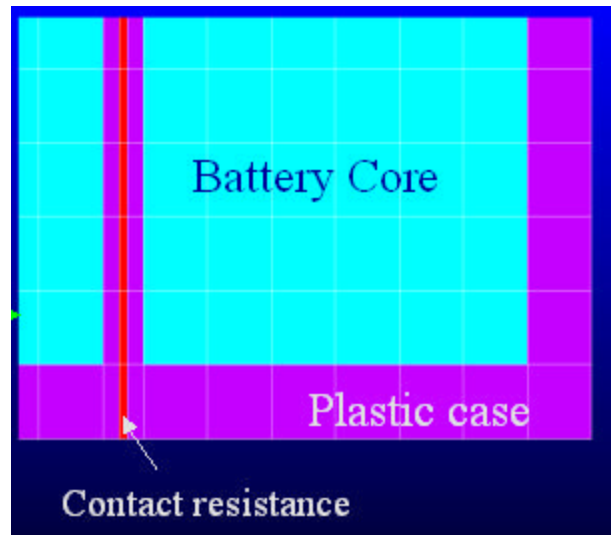


Figure 2. Finite element model detail for Case 1

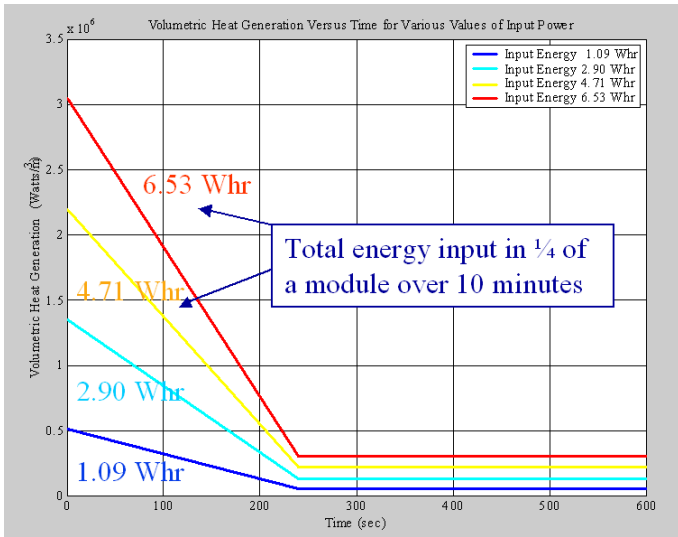


Figure 3. Transient volumetric heat generation

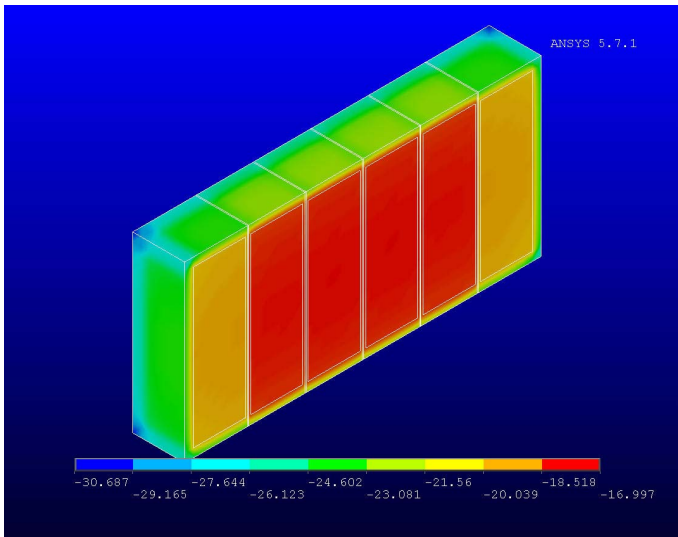


Figure 4. Case 1 temperature distribution at 10 min

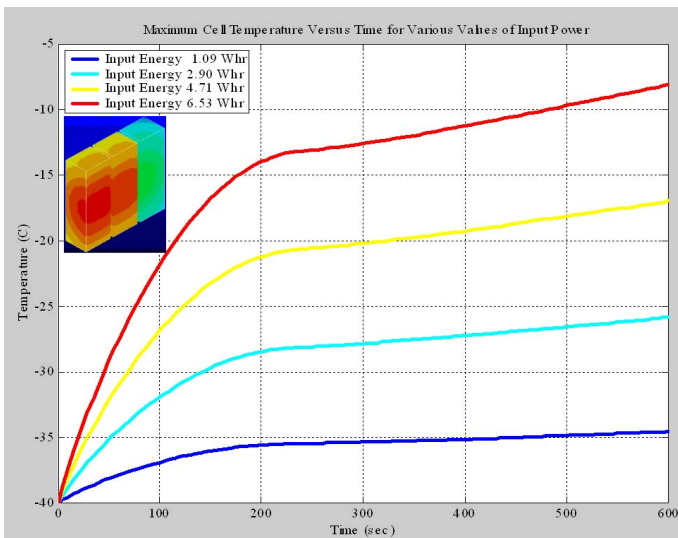


Figure 5. Case 1 maximum cell temperature vs. time

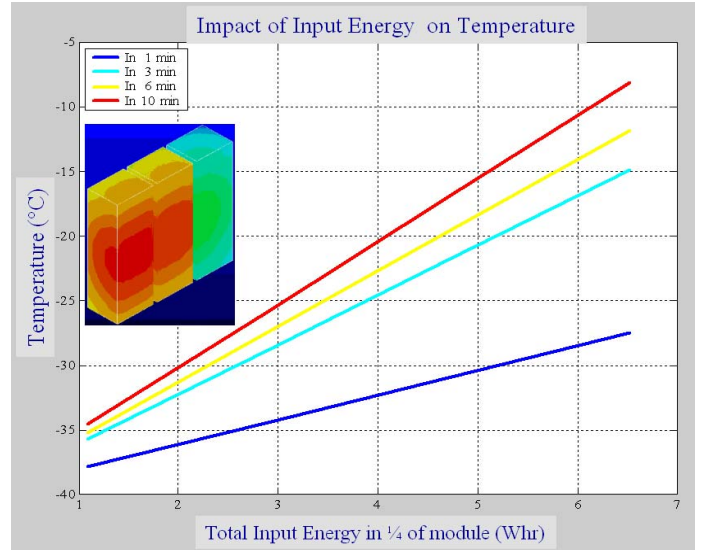


Figure 6. Effect of input energy on temperature rise

CASE 2: EXTERNAL JACKET HEATING

In Case 2, an external jacket heating method using electric heaters around each module was modeled. The geometry of the battery pack considered for this case remains the same as that of Case 1. The thickness of the electric jacket heater was assumed to be 1.7 mm and the insulation thickness was assumed to be 1.7 mm. Figure 7 shows a detail of the Case 2 finite element model with part of the core, plastic case, contact resistance spacer, insulation pad, and heating jacket. Figure 3 shows the transient volumetric heat generation applied at the electric jacket versus time for four different power levels. Natural convection was applied on all exterior surfaces. The heat transfer or convection film coefficient for the side surfaces was assumed to be 2.0 W/m² K. The film coefficient for the top surfaces was assumed to be 3.0 W/m² K.

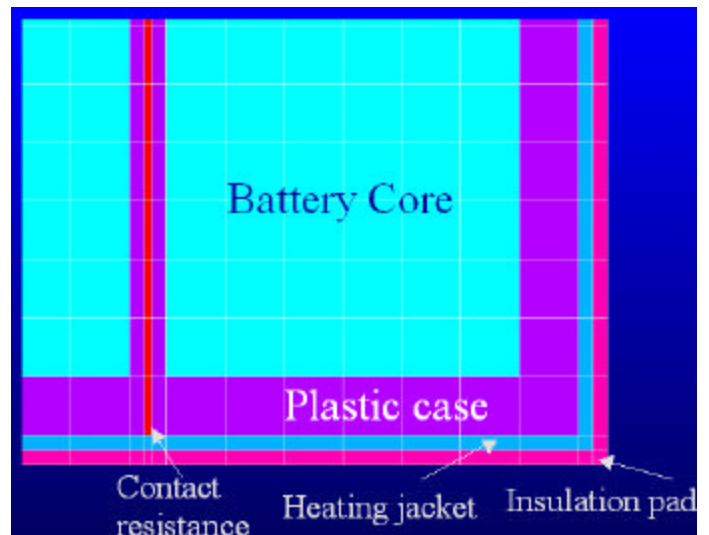


Figure 7. Finite element model detail for Case 2

The film coefficient for the bottom surfaces was assumed to be $1.0 \text{ W/m}^2 \text{ K}$. The environment (bulk temperature for all convection surfaces) and initial module temperature were considered to be -40°C .

Temperature increases with time and the amount of internal heating energy. Figure 8 shows a nonuniform temperature distribution at 10 minutes. The exterior cells are warmer than the interior ones and heat does not get into the battery core easily.

For an input power level of 2.90 Wh the temperature at the top, middle, and bottom points of the exterior cell versus time is shown in Figure 9. Figure 10 shows the core temperature range versus time for an input power level of 6.53 Wh . The maximum and minimum core temperatures, as well as their difference, increase versus time. The same conclusion can be made for all four cases of the input power levels considered.

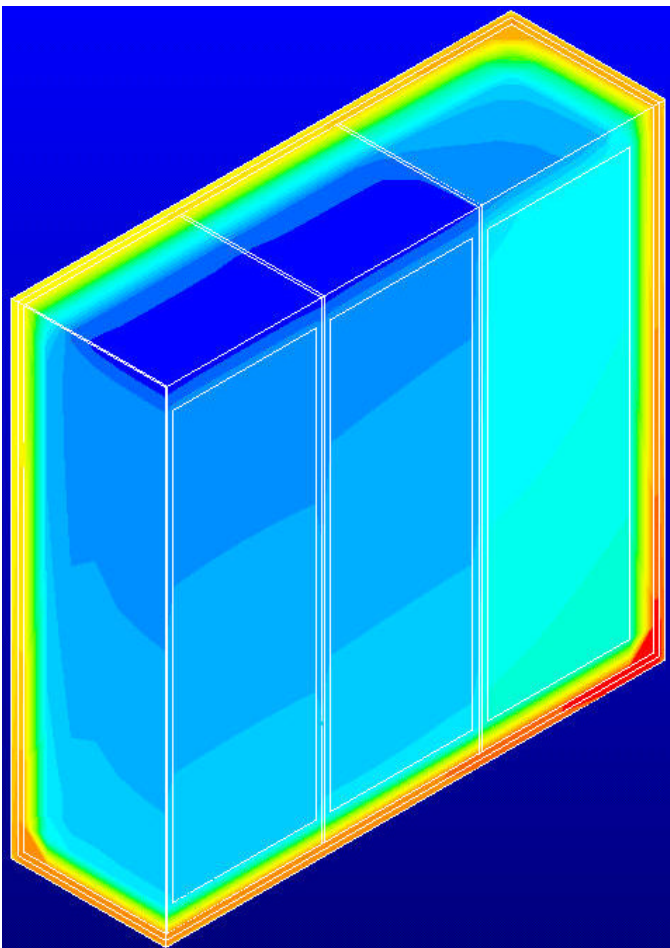


Figure 8. Case 2 temperature distributions at 10 min

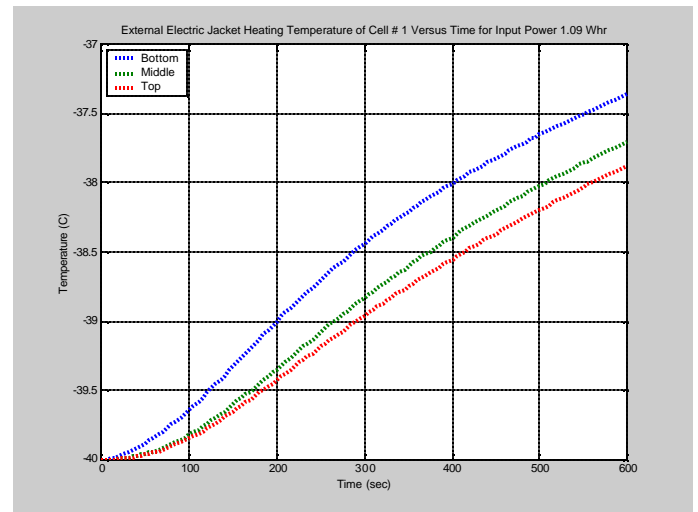


Figure 9. Case 2 temperature of exterior cell vs. time for input power of 2.90 Wh

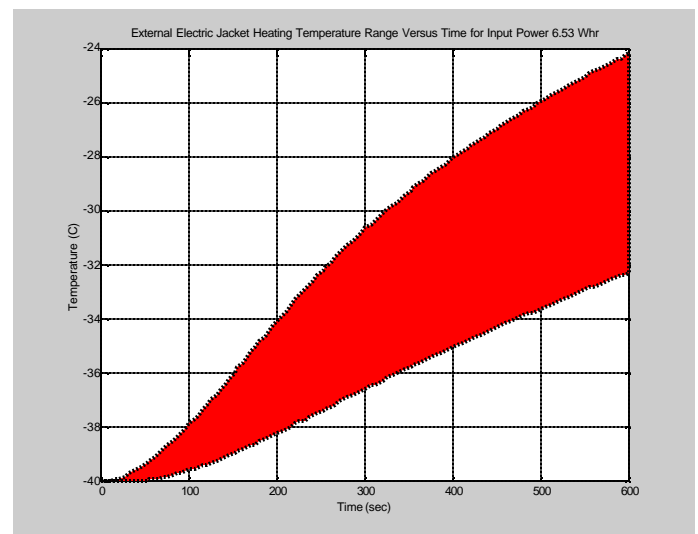


Figure 10. Core temperature range versus time for input power 6.53 Wh

CASE 3: INTERNAL JACKET HEATING

In Case 3, an internal jacket heating method using electric heaters around each cell was modeled. The geometry of the battery pack considered for this case remains the same as that of Case 1. The thickness of the electric jacket heater was assumed to be 1.7 mm and the insulation thickness was assumed to be 1.7 mm . Figure 11 shows a detail of the Case 2 finite element model with a portion of the core, plastic case, insulation pad, and heating jacket. A heating jacket has replaced the contact resistance spacer of the previous case.

Natural convection was applied on all exterior surfaces. The heat transfer or convection film coefficient for the side surfaces was assumed to be $2.0 \text{ W/m}^2 \text{ K}$. The film

coefficient for the top surfaces was assumed to be $3.0 \text{ W/m}^2 \text{ K}$.

The core temperature increases with time and the amount of internal heating energy. Figure 12 shows a nonuniform temperature distribution at 10 minutes. The areas of the interior cells at the corners of the heating pads have higher temperatures. Figure 13 shows the maximum (solid line) and minimum (broken line) core temperature versus time for various input power levels.

The difference between maximum and minimum core temperature increases as the input power level increases. The effect of input energy on temperature rise for 1, 3, 6, and 10 minutes is shown in Figure 14. The temperature rises linearly versus time and the slope increases as the input energy level increases. Figure 15 shows the average temperature versus time for various heating methods at the same power input level. Core electric heating (Case 1) is the most effective technique, followed first by internal jacket heating (Case 3) and then by external jacket heating (Case 4).

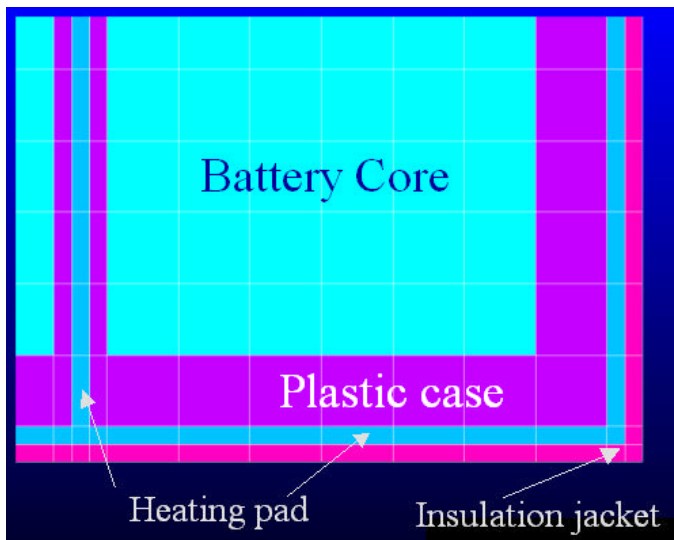


Figure 11. Finite element model detail for Case 3

CASE 4: INTERNAL FLUID HEATING

In Case 4, an internal heating using fluid (air or liquid) around each cell was modeled. The geometry of the battery pack considered for this case remains the same as that of Case 1. The air gap between each cell was assumed to be 1.7 mm. Figure 16 shows a detail of the Case 2 finite element model with part of the core, plastic case, and air gap between each cell. Convection was applied on all exterior surfaces. The heat transfer or forced convection film coefficient for the side surfaces was assumed to be $25.0 \text{ W/m}^2 \text{ K}$. The film coefficient for the top surfaces was assumed to be $5.0 \text{ W/m}^2 \text{ K}$. Based on heat transfer calculations, the air temperature at the inlet (top of the cell) was estimated to be -5.0°C ; and

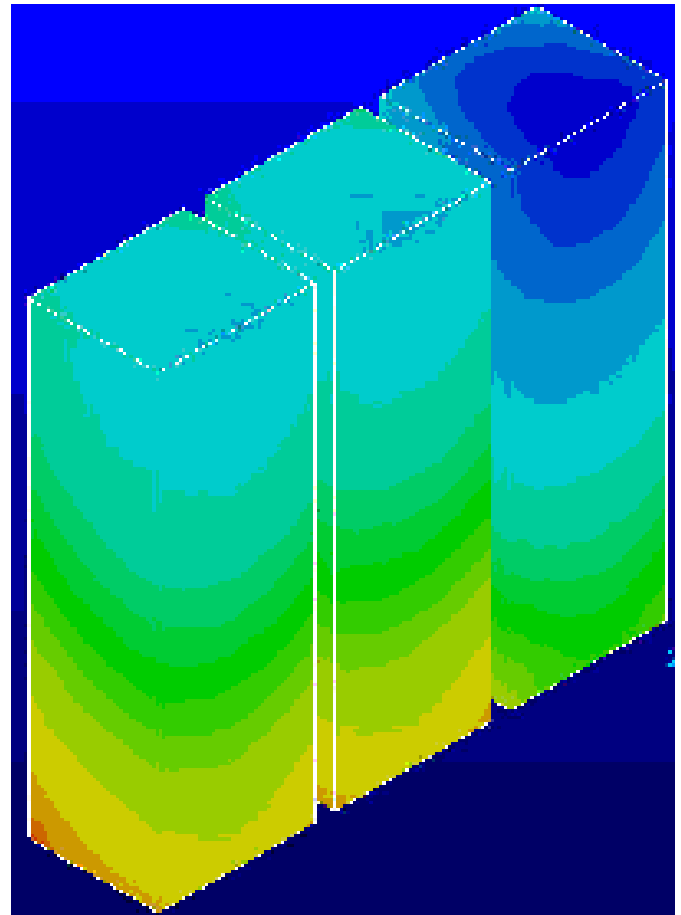


Figure 12. Case 3 temperature distributions at 10 min

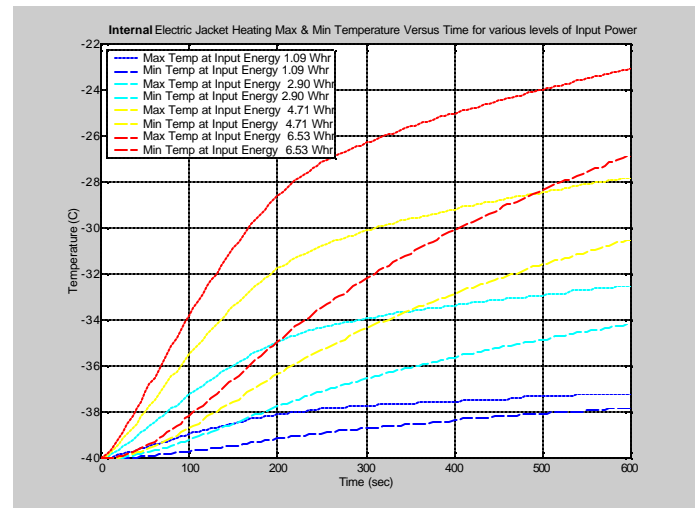


Figure 13. Maximum and minimum core temperature vs. time for various input power levels

based on energy balance the air temperature at the outlet (bottom of the cell) was estimated to be -10.0°C . A linear temperature variation was considered from the top to the bottom of all cells. Temperature increases with time and amount of internal heating energy. Figure 17 shows a nonuniform temperature distribution at 10 minutes of one-

half of a typical cell. The areas at the corners on the top of the cell (inlet of warm air) have higher temperatures.

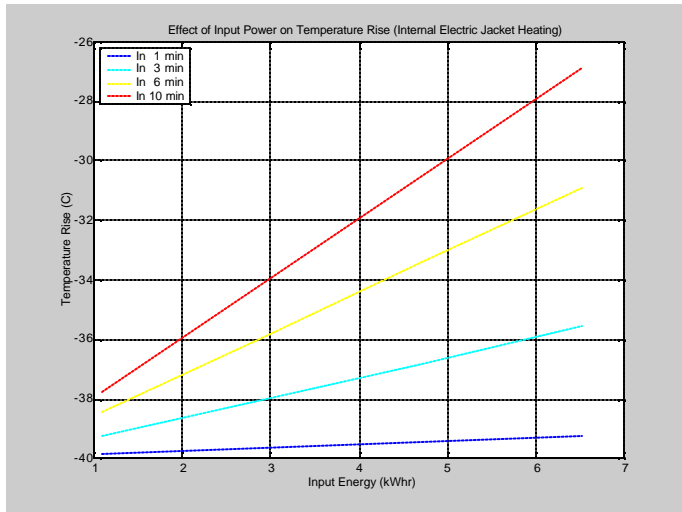


Figure 14. Effect of input energy on temperature rise

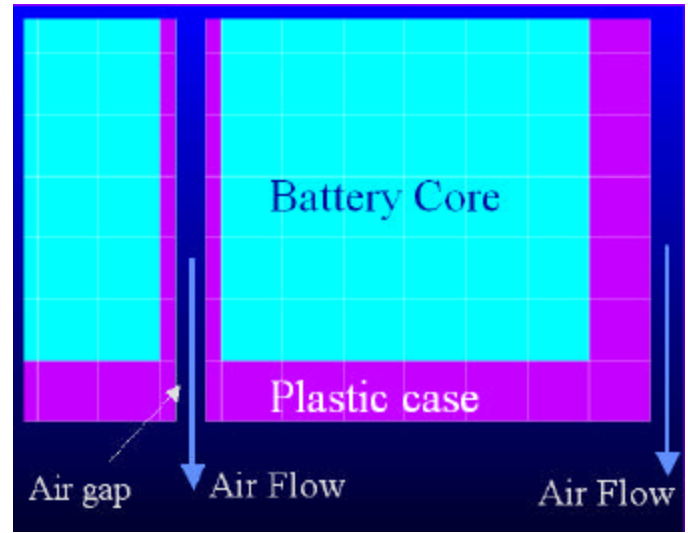


Figure 16. Finite element model detail for Case 4

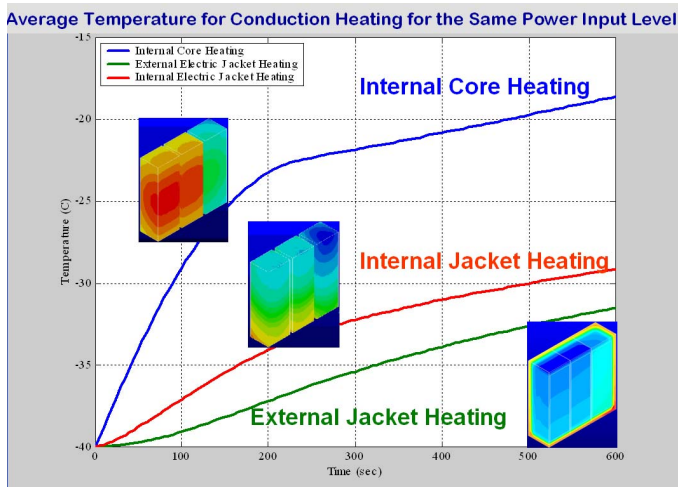


Figure 15. Average temperature vs. time for various heating methods and same power input level

COMPARISON OF THE FOUR CASES

Figure 18 shows the average core temperature at 2 min versus input power for various heating methods. The blue line represents the case of internal heating using battery energy (Case 1). The green line represents the case of external heating using electric heaters (Case 2). The red line represents the case of internal heating using electric heaters (Case 3). The cyan line represents the case of internal airflow heating with 100% efficiency (Case 4 @ 100%) and the purple line represents the case of internal airflow heating with 20% efficiency (Case 4 @ 20%), to indicate heat loss from the fluid system to the environment.

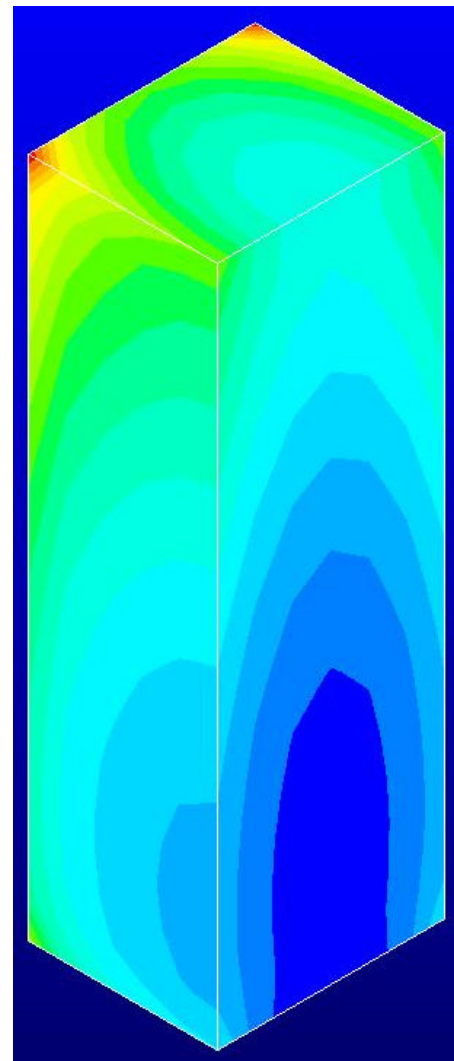


Figure 17. Case 4 Temperature Distribution at 10 min

Figure 19 shows the average core temperature rise at 2 minutes for unit input power of the various heating

methods. The first bar represents Case 1 (internal heating using battery energy), the second bar represents Case 2 (external heating using electric heaters), the third bar represents Case 3 (internal heating using electric heaters), and the fourth bar represents Case 4 @ 100% (internal airflow heating with 100% efficiency).

CORE HEATING TECHNIQUE

After identifying internal core electric heating as the most effective technique, we investigated practical methods to apply it. One method is to apply current to the battery terminals so the resistive heating warms the core. Applying direct current charging may not be feasible because it may cause overgassing at low temperatures. We have worked with the University of Toledo (Stuart and Hande) to utilize core electric heating of lead acid NiMH batteries and using alternating currents (AC).

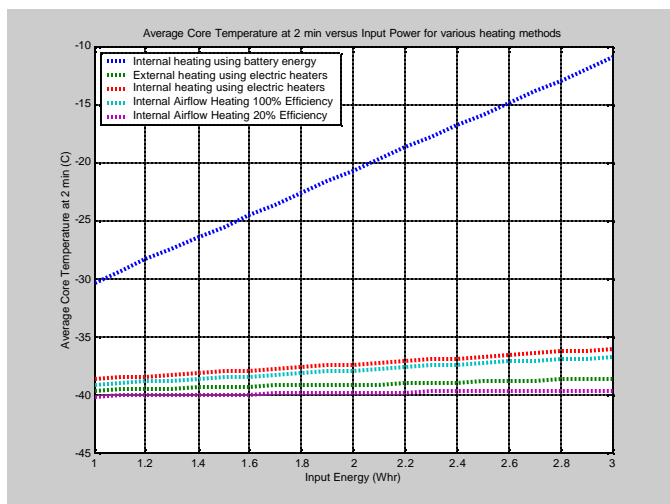


Figure 18. Average core temperature at 2 min vs. input power for various heating methods

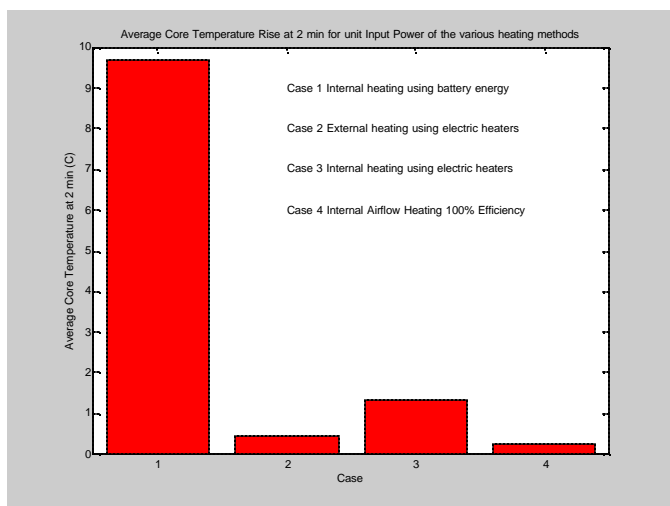


Figure 19. Average core temperature rise at 2 min for unit input power of the various heating methods

Research on AC battery heating is at a very early stage, and many questions remain as to the optimum frequency or effect on battery lifetime and performance. However, initial tests (Pesaran, Vlahinos, and Stuart) have been conducted with batteries at various cold temperatures with different AC currents applied at 60 Hz. The power capability and the available energy of the battery before and after the application of the AC current have been compared. Preliminary tests at -40°C show that a 60 Hz current of 115 Amps can revive an essentially nonoperating 4.9 kg, 1.9 lit, 13 Ah rated VRLA battery in less than 6 minutes. No near-term battery deterioration has been detected, but possible degradation effect is a concern. Possible applications include off-board heaters for EV charging and on-board heaters for HEVs where the AC power is obtained from the generator. Since size and weight are not critical for off-board EV heaters, 60 Hz AC can be used to provide a simple and convenient power source. An on-board HEV heater, however, will require a high frequency (20 kHz) inverter to reduce size and weight. The on-board generator that is driven by the HEV's heat engine would supply power for this inverter. Work on applying high frequency alternating currents for warming a NiMH battery pack was initiated recently.

CONCLUSIONS

From this study the following conclusions can be drawn:

- Electric heating raises the battery temperature faster than heating with fluids.
- The most uniform heating was achieved with internal core heating. (Case 1)
- Among the three electric heating methods core heating (Case 1) reached a much higher temperature sooner than the other heating techniques for the same amount of energy.
- External jacket heating (Case 2) had the largest temperature spread.
- There was slow warm-up time with heating from the outside, particularly with the external electrical jacket heating. (Case 2)
- The best approaches in order of energy efficiency (and without considering cost, packaging, and manufacturing issues) are:
 1. Internal core heating with resistive heating
 2. Internal cell heating using electric jackets heaters
 3. Internal fluid heating around each cell
- Applying AC to battery terminals is feasible way to heat the battery core.
- Future work will involve thermal analysis of battery modules with different shape and material properties and packs.

ACKNOWLEDGMENTS

The Department of Energy (DOE) Office of Advanced Transportation Technologies as part of the Hybrid Propulsion Vehicle Systems Program funded this work. We wish to thank Robert Kost (DOE Vehicle Systems team leader) and Terry Penney (NREL Vehicle Systems technology manager) for their support of this project. We also wish to thank Dr. Tom Stuart of the University of Toledo for providing the results on AC heating of batteries.

REFERENCES

1. Pesaran, A.A., Vlahinos, A., and Burch, S.D., "Thermal Performance of EV and HEV Battery Modules and Packs," in *Proceedings of the 14th International Electric Vehicle Symposium*, Orlando, FL, December 15–17, 1997.
2. Ashtiani, C. and Stuart, T., "Circulating Current Battery Heater," U.S. Patent 6,259,229, July 10, 2001.
3. Stuart, T. and Hande, A., "AC Battery Heating for Cold Climates," presented at EnV 2001 Conference, Engineering Society of Detroit, Southfield, MI, June 10–13, 2001.
4. Pesaran, A., Vlahinos, A., and Stuart, T., "Evaluation of Heating Methods for HEV batteries for Cold Seasons," NREL Milestone Report, August 2001, National Renewable Energy Laboratory.

CONTACTS

Dr. Andreas Vlahinos is principal of Advanced Engineering Solutions, LLC, *your virtual resource for rapid new product development* and professor adjunct at CU-Boulder. He received his Ph.D. in engineering science and mechanics from the Georgia Institute of Technology. He has been professor of structural engineering at the University of Colorado and taught courses in structural

mechanics and computer aided structural engineering. He has received the Professor of the Year Award. He has more than 70 publications in the areas of structural stability, vibrations, structural dynamics, and design optimization. He has received the R&D 100 award and holds several patents. He has been instrumental in rapid product development by implementing Six Sigma and Computer Aided Concurrent Engineering for several government agencies such as NASA, NREL, and DOE and industry partners such as IBM, Coors, Lockheed Martin, Alcoa, Allison Engine Comp., Solar Turbines, Ball, Futech, American Standard, TDM, PTC, MDI, and FORD. Dr. Vlahinos' phone is (303) 814-0455 and his e-mail address is andreas@aes.nu

Dr. Ahmad Pesaran is the Battery Thermal Management team leader at NREL. He holds a B.S. in chemical engineering from Shiraz University, an M.S. in engineering (emphasis on heat and mass transfer), and a Ph.D. in mechanical engineering from UCLA. His master's and Ph.D. research projects centered on experimental and theoretical aspects of heat and moisture transport into porous desiccant particles. He has been involved in various types of energy research including alternative air conditioning for buildings and vehicles, ocean thermal energy conversion, solar buildings, and batteries for hybrid vehicles. He received the R&D 100 award in 2001. Dr. Pesaran has led the effort to develop NREL's battery thermal management capabilities and test facility for the Hybrid Electric Vehicle Program with industry. Dr. Pesaran's phone is (303) 275-4441 and his e-mail address is ahmad_pesaran@nrel.gov.

ADDITIONAL SOURCES

For more information, visit NREL's battery thermal management and assessment Web site at <http://www.ctts.nrel.gov/BTM/>.